Reviewer #1

Thank you for the comments. I provide feedback on each of your comments below. Note that the algorithm has been modified in the revised paper. We wanted to simply the algorithm based Reviewer #2 comments. Therefore, we kept the "most powerful" tests in the algorithm and removed the ones that were having little impact on the results. In the new algorithm we made slight adjustments to the thresholds used for the "most powerful" tests based on the many samples of clear sky, volcanic ash, and cloud that we analyzed. This new, simplified algorithm produces more accurate results than the previous, very complex algorithm. For instance, the previous algorithm allowed too many cloud edges to be identified as ash. We made the thresholds stricter for ash detection in the new algorithm which helps mitigate the cloud edge issue. Also, our new algorithm is capable of detecting thick ash over cloud.

Detailed Comments

Pg. 5578

Line 7: I made the necessary modifications. I rewrote to say **when the solar zenith angle is lower than about 65°.**

Line 25: I use the **Gudmundsson et al. (2013)** reference.

Pg. 5579

Line 1/3: I removed the word **dense**

Line 7: Removed **deadly**

Line 26: Added **thick**

Pg. 5580

Line 3: Fixed misspelling

Line 15: Included reference to Prata and Prata (2012)

Line 24: Not quite sure what you meant here so we made no changes.

Pg. 5586

Line 3-5: Discussed later so ignored here

Line 24: Changed to every 5 minutes

Line 10 onwards: It probably could be modeled quite well. We do not take that approach here but it would be interesting.

Pg. 5588

I made major changes at this point which I believe answer most, if not all, of your comments. I did change the Ackerman reference to Prata (1989) and included a statement about the time validity of our algorithm. This statement is as follows:

The use of the 0.6 μm channel means that our algorithm can only be used during the daylight hours which can be problematic at high latitudes during the winter months where daylight is unavailable.

Pg. 5590

Line 1-2: We now rely on many examples as discussed in the following lines added to the paper:

We **carefully hand picked 28 samples representing volcanic ash, cloud, and clear sky ocean and land surfaces. We do not show a typical dust RGB (e.g. Francis et al., 2012) in Fig. 1 because regions of cloud can be difficult to visually separate from the underlying surface in the dust RGB. Instead, the RGB image in Fig. 1 was produced by assigning the BTD 12.0-10.8 values as the red component, the 0.6 μm reflectance as the green component, and the BTD 10.8-8.7 as the blue component. By using the 0.6 μm channel we could more easily see where small scale clouds were located over both land and ocean allowing us to pick better samples. Note that we also hand picked 28 samples on two other days during the Eyjafjallajökull volcanic eruption period, 7 May at 1100 UTC and 18 May at 1600 UTC. Overall, we hand picked 18 samples of ash over water, 6 samples of ash over land, 30 samples of cloud, and 30 samples of clear sky ocean and land.**

Line 7: Yes, you are correct that this test can be incorrect in some circumstances. We kept this test in our algorithm but included the BTD 10.8-12.0 test along with it (i.e. Table 2). The inclusion of the BTD 10.8-12.0 test will prevent many of these circumstances from occurring since the BTD 10.8-12.0 of fresh, opaque ash clouds are often strongly negative as revealed in the panels in Fig. 3.

Line 18 onwards: Ash absorption at 8.7 μm helps influence a more negative BTD 8.7-10.8. This is shown in Fig. 3b as the many of the fresh, opaque ash clouds have BTD 8.7-10.8 < -4 K which means that this particular threshold test (BTD 8.7-10.8 > -2 K and BTD 10.8-12.0 > 0 K

indicates cloud) is appropriate for ash detection. Note that we included a statement similar to this in the text:

The BTD 8.7-10.8 will vary with ash composition and SO_2 amount in the volcanic cloud which explains the variation in the values in Fig. 3b. In particular, SO_2 absorption at 8.7 μm leads to a decrease or more negative BTD 8.7-10.8 value. The BTD 10.8-12.0 will vary with ash composition, particle sizes, and atmospheric water vapor content. For example, it is generally more difficult to detect ash in regions of high water vapor content where the BTD 10.8-12.0 may be close to zero or positive.

Section 3.5: I added a discussion along with a plot that goes a little further in depth about the time of day. Please see revised paper for the plot (Fig. 2c). Here is the text I added to Section 3.2:

The use of the 0.6 μm channel means that our algorithm can only be used during the daylight hours which can be especially problematic at high latitudes during the winter months where daylight is unavailable. Also, the variation in solar zenith angle during the daylight hours can further restrict the time validity of our algorithm. In order to highlight the change in reflectivity that occurs due to the solar zenith angle, we show the 0.6 μm reflectivity for a clear sky pixel over the water on 5 May 2010 from 1000 to 1800 UTC (Fig. 2c). The 0.6 μm reflectivity values remain rather consistent at around 6% until from 1000 to 1600 UTC even though the solar zenith angle varies from 40° to 62°. However, considerable increases in reflectivity occur after 1600 UTC, especially from 1700 to 1800 UTC where the solar zenith angles are about 70° and 79°, respectively, and the reflectivity of the clear sky pixel increases from 8% to 13.5%. Therefore, our algorithm should not be used when the solar zenith angle is greater than about 65°. In fact, our algorithm results changed rather drastically when advancing in time from 1600 to 1700 UTC for the volcanic ash cases during April and May due to the large increase in reflectivity that occurs when the solar zenith angle is large.

Pg. 5595

Line 19: I removed this sentence.

Line 23: Completely removed the sentence with the inappropriate reference.

Pg. 5596

Line 15 onwards: We actually completely removed this entire case. We show results for another case instead. The 19 April case is a very difficult case with primarily thinner ash over land. The substantial cloud cover among the ash over land made this case even more difficult. Therefore, the 19 April case was not good to show. However, the figure below shows the new results for

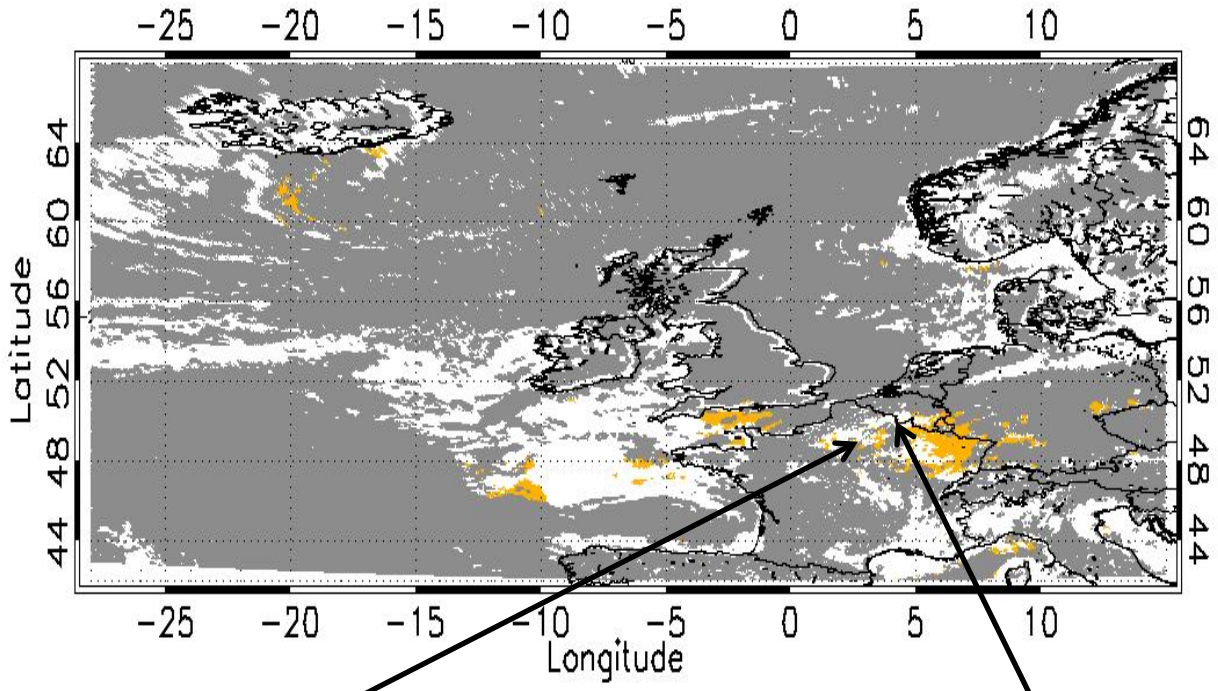

the 19 April case when using our modified algorithm presented in the revised paper. The previous version of the algorithm identified many areas as ash that were not detected by neither MODIS or MISR. These areas may have been false identifications. The new algorithm results here show that many of those possible false detections have vanished and have now been identified as cloud, which is mostly due to the fact that our new algorithm has slightly different thresholds to detect clouds. The slight change in thresholds help to properly identify most cloud edges as cloud. Our previous algorithm tended to identify cloud edges as ash. Furthermore, our new algorithm still shows the ash over Europe. This ash appears to be real according to cloud-screened AERONET data on this day.

You can see from the above AERONET data at Paris and Brussels on 19 April 2010 that AOD at 440 nm was about 0.48 and 0.37, respectively. These are rather low AOD amounts but the AERONET data still suggests that aged ash was in the area. Furthermore, the ash identifications further to the west over water are very difficult to validate but MODIS AOD suggests that aerosol was present in this region. However, it is possible that our algorithm is identifying some areas near cloud edges as aerosol.

Note that our algorithm will detect other aerosol types as well, especially dust aerosol since it influences negative BTD 10.8-12.0. However, for this volcanic eruption period, ash was the dominant aerosol signal.

Pg. 5598

This 17 May case study remains in the paper but the results have changed since the newest version of the algorithm. Also, note that we use FAAM aircraft data to validate our results later in this section. The FAAM indicates that ash was present across the regions where our algorithm detects ash. But, we show that the FAAM retrieves fairly low AOD during portions of its flight

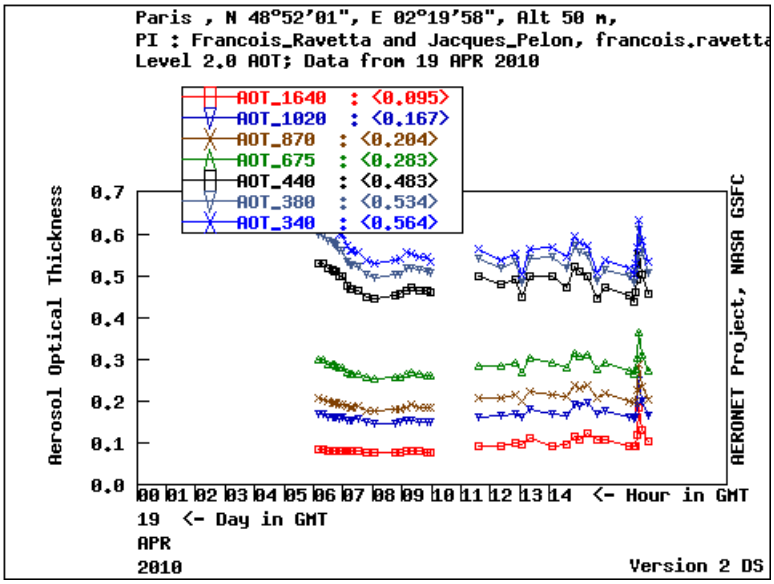

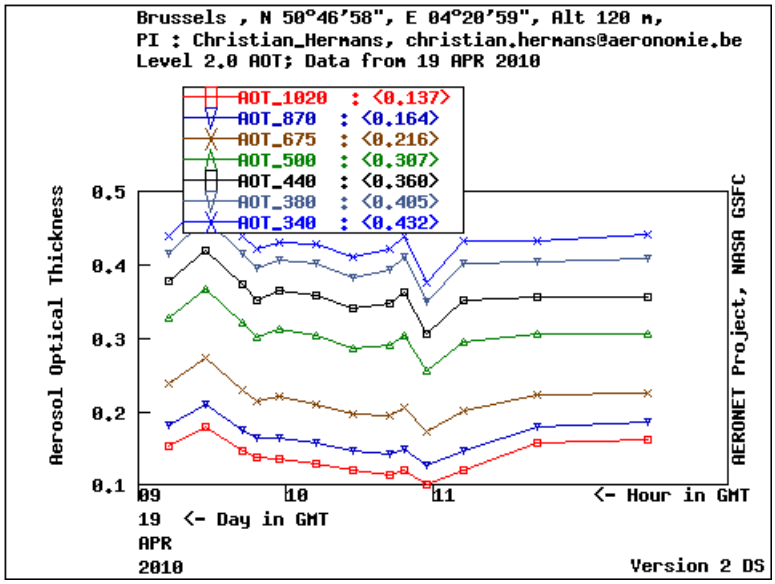

which indicates low concentrations of ash that pose no threat to aviation. Please refer to Marenco et al. (2011) who also analyze the 17 May case in detail using FAAM and model simulations. In their paper, both the FAAM and model simulations show that ash was in fact present across the areas where our algorithm detects ash. Again, they showed that ash concentrations were low at times according to both the FAAM and model simulations which suggests that our algorithm will detect these lower concentrations of ash which pose no threat to aviation. Here is the new text added to the revised paper (Bold text represents new text):

Figs. 5a-f are similar to Figs. 4a-f except that the former pertain to the 17 May 2010 case study at 1300 UTC where a significant area of volcanic ash resided over the North Sea around 56°N and 7°W (Turnbull et al., 2012). **This ash plume is not as apparent on the SEVIRI dust RGB due to the fallout of ash particles during its transport from Iceland. In fact, it is difficult to decipher the ash plume from the low level clouds (yellowish colors) across the domain. Analyzing both the dust RGB and visible image along with the BTD 10.8-12.0 map (i.e. Fig. 5c) helps better understand where the potential ash regions are located. The pink to yellow colors associated with the ash plume in the dust RGB appear darker than the whiter clouds in the visible image across the North Sea. By this time, the ash plume has become only slightly more reflective than the background ocean. There are some clouds among the ash plume that are only noticeable when closely inspecting the visible image which shows the utility of analyzing both the dust RGB and visible image. The BTD 10.8-12.0 map shows a considerable area over the North Sea and Norwegian Sea that has BTD 10.8-12.0 < -1 K suggesting that ash is present across the area. Our algorithm is easily able to identify these areas where the BTD 10.8-12.0 < -1 K and thick ash is likely present.** According to the dust RGB and visible image, our algorithm successfully disregards cloud contaminated areas within the ash plume region over the North Sea. For example, clouds are shown off the coast of the Netherlands (~56°N, 5°E) and this area is labeled as cloud by our algorithm. **Overall, our algorithm appears to identify clouds very well across the domain which is critical as the final aerosol spatial distribution maps depend on the success of the cloud detection. Moreover, our algorithm identifies aerosol in locations across the North Sea that have BTD 10.8-12.0 > 0 K and appear to be cloud-free. These results are in fairly good agreement to the spatial distribution of MODIS AOD across the North Sea which implies that our algorithm is performing accurately on this day. MODIS retrieves AOD primarily ranging from 0.2 to 0.4 across the North Sea with the exception of a few higher AOD regions where values near 0.7 are present. The location of the higher AOD regions coincide with BTD 10.8-12.0 < -1 K while the AOD from 0.2 to 0.4 coincide with near zero to positive BTD 10.8-12.0 values. The MISR AOD agrees fairly well with MODIS in the limited locations of MISR availability over the North Sea and Norwegian Sea which gives us better confidence that the MODIS retrievals are good on this day. Although our algorithm is able to detect these areas of optically thinner ash identified by MODIS and**

MISR, it is likely that they are below the mass concentration threshold of 0.2 g m^{-2} and do not pose a threat to aviation (Francis et al., 2012; Prata and Prata, 2012). Again, our algorithm mostly misses the very low AOD regions below about 0.2 that are detected by MODIS and MISR. For example, our algorithm labels the area just north of Great Britain as clear sky while the MISR and MODIS retrieves AOD around 0.15. Finally, note that our algorithm is able to detect the thick ash over the Norwegian Sea (~64°N, 0°E) even though it is above a considerable area of clouds according to the SEVIRI visible image. Once again, this shows the ability of our algorithm to detect thick ash above cloud which can pose a threat to aviation.

The studies of Francis et al. (2012), Prata and Prata (2012), and Marenco et al. (2011) all analyze this 17 May volcanic ash event over the North Sea. Our algorithm detects a much broader area of volcanic ash over the North Sea than shown in Francis et al. (2012) and Prata and Prata (2012). The SEVIRI retrieval algorithms developed in these two studies rely heavily on the BTD 10.8-12.0 approach to detect ash. However, ash is not always associated with BTD 10.8-12.0 < 0 K, especially thinner ash regions (AOD < 0.5). These two studies use FAAM BAe146 aircraft data to validate their results. In particular, Francis et al. (2012) show that their algorithm is able to detect the 17 May ash plume where ash concentrations from the FAAM aircraft are greater than about 0.3 g m^{-2}. However, when FAAM ash concentrations drop below about 0.3 g m^{-2} their algorithm fails to detect any ash. The FAAM aircraft actually retrieves ash concentrations all the way to the eastern coast of Great Britian which our algorithm is able to detect (i.e. Fig. 5d). Thus, it appears that our algorithm is capable of detecting more ash compared to the algorithms in Francis et al. (2012) and Prata and Prata (2012). However, the ash areas that are undetected in these two studies have fairly low concentrations (less than about 0.3 g m^{-2}) and may not pose any threat to aviation. Marenco et al. (2011) perform modeling simulations of this volcanic ash event where the model shows a broad area of ash over the North Sea. In fact, the area of ash simulated by the model is even larger than the broad area identified by our algorithm.

Added Section:

In order to provide further validation for our algorithm, we perform a validation experiment in Section 4.3:

4.3 Validation experiment

In order to obtain a better understanding of the accuracy of our SEVIRI algorithm, we perform an additional experiment where we choose 28 samples for three different days and times (i.e. 7 May at 1100 UTC, 11 May at 1300 UTC, and 18 May at 1600 UTC) during the Eyjafjallajökull volcanic eruption period. These "truth" samples were chosen by examining the dust RGB images along with visible and infrared images, and carefully picking areas of clear sky, volcanic ash, and clouds. Note that these samples are different from the ones chosen earlier in this study that helped set the thresholds for the tests in our algorithm. Then, we run our algorithm for these three different days and check the results against the "truth" samples. An example of the 28 samples chosen for the 7 May at 1100 UTC case is shown in Fig. 8a where boxes 1-4 are clear sky ocean, 5-12 are volcanic ash, and 13-28 are clouds. We had very limited clear sky land pixels available on this day which explains why we did not choose any samples of clear sky land. The 84 samples taken on these three days represent the truth. Then, we run our SEVIRI algorithm for these three cases and compare the results against truth samples. Overall, we picked 30 ash over water samples on these three days which gave a total of 1080 individual ash pixels to compare against our algorithm results as the size of the each sample spanned 6 by 6 boxes. According to the truth samples, the algorithm performed very well as 936 of the 1080 pixels were accurately labeled as ash by our algorithm giving a success rate of 87%. Not surprisingly, our algorithm performed even better with identifying clouds. Overall, the 60 samples of clouds that we picked provided us with 2160 individual cloud pixels as truth. Our algorithm successfully labeled 2127 of these truth pixels as cloud which gives a 98% success rate for cloud identification. Of course, when performing a validation experiment where we are carefully hand picking "truth" samples, it is easy to make an algorithm appear more accurate than reality by choosing samples that should be easy for the algorithm to handle. For this validation experiment, we chose samples that, in our opinion, have a wide range of difficulty for the algorithm to identify. Finally, we present the

SEVIRI algorithm results for the 7 May at 1100 UTC case where the majority of the ash plume is accurately labeled by the algorithm. This is another case where ash resided above clouds which can make it difficult to identify the ash due to the presence of the cloud. In fact, our algorithm is not able to identify the full extent of the ash plume since the BTD 10.8-12.0 values increase to near or above 0 K. As a result, our algorithm recognizes parts of the ash plume as cloud.

Reviewer #2

Thank you for the comments. I provide feedback on each of your comments below. Note that the algorithm has been modified in the revised paper. We wanted to simply the algorithm based on your comments. Therefore, we kept the "most powerful" tests in the algorithm and removed the ones that were having little impact on the results. In the new algorithm we made slight adjustments to the thresholds used for the "most powerful" tests based on the many samples of clear sky, volcanic ash, and cloud that we analyzed. This new, simplified algorithm produces more accurate results than the previous, very complex algorithm. For instance, the previous algorithm allowed too many cloud edges to be identified as ash. We made the thresholds stricter for ash detection in the new algorithm which helps mitigate the cloud edge issue. Also, our new algorithm is capable of detecting thick ash over cloud.

General Comments

Please see the revised paper where the bold text indicates new text.

#1: We simplified the algorithm and have chosen a much larger number of samples that helped set the thresholds in the algorithm.

#2: We have highlighted this major limitation of the algorithm in the revised paper. For instance, in the revised paper we added the following text.

The use of the 0.6 μm channel means that our algorithm can only be used during the daylight hours which can be especially problematic at high latitudes during the winter months where daylight is unavailable. Also, the variation in solar zenith angle during the daylight hours can further restrict the time validity of our algorithm. In order to highlight the change in reflectivity that occurs due to the solar zenith angle, we show the 0.6 μm reflectivity for a clear sky pixel over the water on 5 May 2010 from 1000 to 1800 UTC (Fig. 2c). The 0.6 μm reflectivity values remain rather consistent at around 6% until from 1000 to 1600 UTC even though the solar zenith angle varies from 40° to 62°. However, considerable increases in reflectivity occur after 1600 UTC, especially from 1700 to 1800 UTC where the solar zenith angles are about 70° and 79°, respectively, and the reflectivity of the clear sky pixel increases from 8% to 13.5%. Therefore, our algorithm should not be used when the solar zenith angle is greater than about 65°. In fact, our algorithm results changed rather drastically when advancing in time from 1600 to 1700 UTC for the volcanic ash cases during April and May due to the large increase in reflectivity that occurs when the solar zenith angle is large.

#3: We have included text where we discuss the Francis et al. (2012) and Prata and Prata (2012) retrieval algorithm results in the revised paper:

The studies of Francis et al. (2012), Prata and Prata (2012), and Marenco et al. (2011) all analyze this 17 May volcanic ash event over the North Sea. Our algorithm detects a much broader area of volcanic ash over the North Sea than shown in Francis et al. (2012) and Prata and Prata (2012). The SEVIRI retrieval algorithms developed in these two studies rely heavily on the BTD 10.8-12.0 approach to detect ash. However, ash is not always associated with BTD 10.8-12.0 < 0 K, especially thinner ash regions (AOD < 0.5). These two studies use FAAM BAe146 aircraft data to validate their results. In particular, Francis et al. (2012) show that their algorithm is able to detect the 17 May ash plume where ash concentrations from the FAAM aircraft are greater than about 0.3 g m^{-2}. However, when FAAM ash concentrations drop below about 0.3 g m^{-2} their algorithm fails to detect any ash. The FAAM aircraft actually retrieves ash concentrations all the way to the eastern coast of Great Britian which our algorithm is able to detect (i.e. Fig. 5d). Thus, it appears that our algorithm is capable of detecting more ash compared to the algorithms in Francis et al. (2012) and Prata and Prata (2012). However, the ash areas that are undetected in these two studies have fairly low concentrations (less than about 0.3 g m^{-2}) and may not pose any threat to aviation. Marenco et al. (2011) perform modeling simulations of this volcanic ash event where the model shows a broad area of ash over the North Sea. In fact, the area of ash simulated by the model is even larger than the broad area identified by our algorithm.

Note that we also discuss the Pavolonis et al. (2006) study in the introduction. We also fixed the issue with repeating image captions in the paper.

#4: We no longer carry out three separate classification tests. Please refer to the new algorithm in the revised paper.

#5: Our new algorithm now uses the past 14 days of data to generate the clear sky reflectance maps in order to make it valid in operational situations. We include a new figure where we look at the clear sky reflectance of a water pixel (Fig. 2c). We also show a bispectral plot with σT 1.6 μ (Fig. 3d) to highlight the ability of the temporal test.

Specific Comments

1. Changed reference to **Gudmundsson et al. (2013)**

2. Added reference Christopher et al. (2011) and reworded sentence.

3. We were just mentioning the RGB images as a tool to understand the spatial distribution of volcanic ash. We discuss the BTD 10.8-12.0 approach to map ash beginning Line 114 on Page 4 of the revised paper.

4. We realized this a major flaw in the algorithm. We have since modified the algorithm to mitigate this issue.

5. Using the minimum 0.6 μm over bright surfaces such as desert causes problems since absorbing cloud and aerosols over desert can actually have lead to a lower 0.6 μm reflectance at the TOA than under clear sky desert conditions. Therefore, over bright surfaces only, we find the highest BT 10.8 value since the highest BT 10.8 over a 14 day period will generally occur in clear sky conditions. Then, we find the 0.6 μm reflectance of this pixel with the highest 10.8 μm value. As a result, the 0.6 μm reflectance value used over desert surfaces will truly represent clear sky conditions.

6. This limitation no longer exists.

7. We added the following text to the revised paper:

For example, Fig. 1 is a SEVIRI RGB image on 17 May 2010 at 1330 UTC over Europe and the Atlantic Ocean where we **carefully hand picked 28 samples representing volcanic ash, cloud, and clear sky ocean and land surfaces. We do not show a typical dust RGB (e.g. Francis et al., 2012) in Fig. 1 because regions of cloud can be difficult to visually separate from the underlying surface in the dust RGB. Instead, the RGB image in Fig. 1 was produced by assigning the BTD 12.0-10.8 values as the red component, the 0.6 μm reflectance as the green component, and the BTD 10.8-8.7 as the blue component. By using the 0.6 μm channel we could more easily see where small scale clouds were located over both land and ocean allowing us to pick better samples.**

8. We reword this sentence as:

The mean ash reflectivity drops to only about 6% at 1.6 μm mostly due to the fact that ash will typically contain a larger number of smaller particles which influences a decreasing reflectance from the visible to near IR wavelengths (Weber et al., 2012).

9. We no longer use the 3.9 μm channel in the new algorithm.

10. This test is no longer used. Nonetheless, note that in the previous version of the algorithm this BTD 10.8-12.0 test was only applied to pixels that were identified as features. Thus, this test would not be used in clear sky areas.

11. Yes, you are correct that this test can be incorrect in some circumstances. We kept this test in our algorithm but included the BTD 10.8-12.0 test along with it (i.e. Table 2). The inclusion of the BTD 10.8-12.0 test will prevent many of these circumstances from occurring since the BTD 10.8-12.0 of fresh, opaque ash clouds are often strongly negative as revealed in the panels in Fig. 3.

12. We no longer use the BTD 3.9-10.8 test.

13. I think you might have miss-understood this (or maybe we have miss-understood your comment). The temporal tests use 3 successive 15 minute SEVIRI scans to calculate the standard deviation of each pixel for the SEVIRI image centered in the middle of the 3 scans. For instance, in our algorithm, we use a 1.6 μm temporal test where we calculate the standard deviation of the 1.6 μm reflectivity over the 3 successive SEVIRI scans. Then, we use these standard deviation values to decide whether the feature is a cloud. If the pixel fails the test, then it remains labeled as aerosol and continues to the other cloud tests. If the pixel passes the test, then it is labeled as cloud. Temporal tests can lead to overestimation of cloud coverage. For example, if a cloud moves into a pixel by the third successive SEVIRI scan, then this pixel can be labeled as cloud even though it may have been clear sky in the middle SEVIRI scan. We discuss these limitations in the revised paper.

14: We have now derived our thresholds based on many different samples which is explained in the following text of the revised paper.

We **carefully hand picked 28 samples representing volcanic ash, cloud, and clear sky ocean and land surfaces. We do not show a typical dust RGB (e.g. Francis et al., 2012) in Fig. 1 because regions of cloud can be difficult to visually separate from the underlying surface in the dust RGB. Instead, the RGB image in Fig. 1 was produced by assigning the BTD 12.0-10.8 values as the red component, the 0.6 μm reflectance as the green component, and the**

BTD 10.8-8.7 as the blue component. By using the 0.6 μm channel we could more easily see where small scale clouds were located over both land and ocean allowing us to pick better samples. Note that we also hand picked 28 samples on two other days during the Eyjafjallajökull volcanic eruption period, 7 May at 1100 UTC and 18 May at 1600 UTC. Overall, we hand picked 18 samples of ash over water, 6 samples of ash over land, 30 samples of cloud, and 30 samples of clear sky ocean and land.

15: We actually removed this sentence since Reviewer #1 did not find it appropriate for the paper. However, it is not necessarily good that our algorithm will detect dust along with ash. But, this is very difficult to avoid since both ash and dust influence negative BTD 10.8-12.0 and many published retrieval algorithms rely on this test for ash detection. Therefore, these retrieval algorithms (e.g. Francis et al. (2012) and Prata and Prata (2012)) will also detect dust along with ash.

16: We no longer use the phrase "thicker ash" but more concentrated ash. Note that the text in this Section has been heavily modified. The new text for this Section 4.2 now reads:

Figs. 5a-f are similar to Figs. 4a-f except that the former pertain to the 17 May 2010 case study at 1300 UTC where a significant area of volcanic ash resided over the North Sea around 56°N and 7°W (Turnbull et al., 2012). **This ash plume is not as apparent on the SEVIRI dust RGB due to the fallout of ash particles during its transport from Iceland. In fact, it is difficult to decipher the ash plume from the low level clouds (yellowish colors) across the domain. Analyzing both the dust RGB and visible image along with the BTD 10.8-12.0 map (i.e. Fig. 5c) helps better understand where the potential ash regions are located. The pink to yellow colors associated with the ash plume in the dust RGB appear darker than the whiter clouds in the visible image across the North Sea. By this time, the ash plume has become only slightly more reflective than the background ocean. There are some clouds among the ash plume that are only noticeable when closely inspecting the visible image which shows the utility of analyzing both the dust RGB and visible image. The BTD 10.8-12.0 map shows a considerable area over the North Sea and Norwegian Sea that has BTD 10.8-12.0 < -1 K suggesting that concentrated ash is present across the area. Our algorithm is easily able to identify these areas where the BTD 10.8-12.0 < -1 K.** According to the dust RGB and visible image, our algorithm successfully disregards cloud contaminated areas within

the ash plume region over the North Sea. For example, clouds are shown off the coast of the Netherlands (~56°N, 5°E) and this area is labeled as cloud by our algorithm. **Overall, our algorithm appears to identify clouds very well across the domain which is critical as the final ash spatial distribution maps depend on the success of the cloud detection. Moreover, our algorithm identifies ash in locations across the North Sea that have BTD 10.8-12.0 > 0 K and appear to be cloud-free. These results are in fairly good agreement to the spatial distribution of MODIS AOD across the North Sea which implies that our algorithm is performing accurately on this day. MODIS retrieves AOD primarily ranging from 0.2 to 0.4 across the North Sea with the exception of a few higher AOD regions where values near 0.7 are present. The location of the higher AOD regions coincide with BTD 10.8-12.0 < -1 K while the AOD from 0.2 to 0.4 coincide with near zero to positive BTD 10.8-12.0 values. The MISR AOD agrees fairly well with MODIS in the limited locations of MISR availability over the North Sea and Norwegian Sea which gives us better confidence that the MODIS retrievals are good on this day. Although our algorithm is able to detect these areas of optically thinner ash identified by MODIS and MISR, it is likely that they are below the mass concentration threshold of 0.2 g m^{-2} and do not pose a threat to aviation (Francis et al., 2012; Prata and Prata, 2012). Again, our algorithm mostly misses the very low AOD regions below about 0.2 that are detected by MODIS and MISR. For example, our algorithm labels the area just north of Great Britain as clear sky while the MISR and MODIS retrieves AOD around 0.15. Finally, note that our algorithm is able to detect the thick ash over the Norwegian Sea (~64°N, 0°E) even though it is above a considerable area of clouds according to the SEVIRI visible image. Once again, this shows the ability of our algorithm to detect thick ash above cloud which can pose a threat to aviation.**

The studies of Francis et al. (2012), Prata and Prata (2012), and Marenco et al. (2011) all analyze this 17 May volcanic ash event over the North Sea. Our algorithm detects a much broader area of volcanic ash over the North Sea than shown in Francis et al. (2012) and Prata and Prata (2012). The SEVIRI retrieval algorithms developed in these two studies rely heavily on the BTD 10.8-12.0 approach to detect ash. However, ash is not always associated with BTD 10.8-12.0 < 0 K, especially thinner ash regions (AOD < 0.5). These two studies use FAAM BAe146 aircraft data to validate their results. In particular, Francis et al. (2012) show that their algorithm is able to detect the 17 May ash plume where

ash concentrations from the FAAM aircraft are greater than about 0.3 g m^{-2}. However, when FAAM ash concentrations drop below about 0.3 g m^{-2} their algorithm fails to detect any ash. The FAAM aircraft actually retrieves ash concentrations all the way to the eastern coast of Great Britian which our algorithm is able to detect (i.e. Fig. 5d). Thus, it appears that our algorithm is capable of detecting more ash compared to the algorithms in Francis et al. (2012) and Prata and Prata (2012). However, the ash areas that are undetected in these two studies have fairly low concentrations (less than about 0.3 g m^{-2}) and may not pose any threat to aviation. Marenco et al. (2011) perform modeling simulations of this volcanic ash event where the model shows a broad area of ash over the North Sea. In fact, the area of ash simulated by the model is even larger than the broad area identified by our algorithm.

17: We modified the text to say ash and not aerosol. We are not trying to detect all aerosol but our algorithm will detect dust aerosol as well.

18: It is not our intention to detect both dust and ash, but this will typically occur with all retrieval algorithms using satellite measurements as it is very difficult to decipher between the two aerosol types. Nonetheless, we include the following text in the revised paper:

Note that our algorithm is capable of detecting all aerosol types that cause an increase in the 0.6 μm clear sky reflectance values. Consequently, this algorithm should be used along with dust RGB images and other more conventional methods such as the BTD 10.8-12.0 maps during operational situations. Of course, when both ash and dust aerosol are present in a region, then the RGB images and conventional methods will not help separate the aerosol types since both ash and dust generally influence negative BTD 10.8-12.0 values. If our algorithm is used alone in situations where other aerosol types (e.g. smoke) along with ash are present, then aircraft pilots may be falsely alarmed of ash in the area. However, for our particular study period, volcanic ash is the dominant aerosol type throughout the domain which is why we refer to ash throughout the remainder of the paper.

19: Added to revised paper:

For example, Fig. 1 is a SEVIRI RGB image on 17 May 2010 at 1330 UTC over Europe and the Atlantic Ocean where we **carefully hand picked 28 samples representing volcanic ash, cloud,**

and clear sky ocean and land surfaces. We do not show a typical dust RGB (e.g. Francis et al., 2012) in Fig. 1 because regions of cloud can be difficult to visually separate from the underlying surface in the dust RGB. Instead, the RGB image in Fig. 1 was produced by assigning the BTD 12.0-10.8 values as the red component, the 0.6 μm reflectance as the green component, and the BTD 10.8-8.7 as the blue component. By using the 0.6 μm channel we could more easily see where small scale clouds were located over both land and ocean allowing us to pick better samples.

20: We are not relying on one sample anymore.

21: We have included in the revised paper:

The BTD 8.7-10.8 will vary with ash composition and SO_2 amount in the volcanic cloud which explains the variation in the values in Fig. 3b. In particular, SO_2 absorption at 8.7 μm leads to a decrease or more negative BTD 8.7-10.8 value. The BTD 10.8-12.0 will vary with ash composition, particle sizes, and atmospheric water vapor content. For example, it is generally more difficult to detect ash in regions of high water vapor content where the BTD 10.8-12.0 may be close to zero or positive.

22: The RGB is now described in the text and we show the key for the MODIS AOD. We also increased the height of the individual images.

Fig. 4a is a SEVIRI dust RGB image on 13 April 2010 at 1200 UTC when a substantial amount of ash was being emitted from the Eyjafjallajökull volcano. The dust RGB image was produced by assigning the BTD 12.0-10.8 values as the red component, the BTD 10.8-8.7 as the green component, and the BTD 10.8 μm as the blue component (Francis et al., 2012). The volcanic ash is identified in the SEVIRI dust RGB image by the reddish colors extending eastward from Iceland.

Technical corrections were taken care of in revised paper.